Exploring pharmacological inhibition of $G_{q/11}$ as an analgesic strategy

Subhi Marwari,

Cody Kowalski,

Kirill A. Martemyanov[*]

Department of Neuroscience, The Scripps Research Institute, 130 Scripps Way, Jupiter, FL, 33458, USA

Abstract

BACKGROUND AND PURPOSE: Misuse of opioids has greatly affected our society. One potential solution is to develop analgesics that act at targets other than opioid receptors. These can be either used as stand-alone therapeutics or to improve the safety profile of opioid drugs. Previous research showed that activation of $G_{q/11}$ proteins by G protein-coupled receptors has pro-nociceptive properties suggesting that blockade of $G_{q/11}$ signaling could be beneficial for pain control. The aim of this study was to test this hypothesis pharmacologically by using potent and selective $G_{q/11}$ inhibitor YM-254890.

EXPERIMENTAL APPROACH: We used a series of behavioral assays to evaluate the acute responses of mice to painful thermal stimulation while administering YM-254890 alone and in combination with morphine. We then used electrophysiological recordings to evaluate the effects of YM-254890 on the excitability of dorsal root ganglion (DRG) nociceptor neurons.

KEY RESULTS: We found that systemic administration of YM-254890 produced antinociceptive effects and also augmented morphine analgesia in both hot plate and tail flick paradigms. However, it also caused substantial inhibition of locomotion, which may limit its therapeutic utility. To circumvent these issues, we explored the local administration of YM-254890. Intrathecal injections of YM-254890 produced lasting analgesia in a tail flick test and greatly augmented the anti-nociceptive effects of morphine without any significant effects on locomotor behavior. Electrophysiological studies showed that YM-254890 reduced the excitability of DRG nociceptors and augmented their opioid-induced inhibition.

CONCLUSIONS AND IMPLICATIONS: These findings indicate that pharmacological inhibition of $G_{q/11}$ could be explored as an analgesic strategy.

Keywords

GPCR; G proteins; YM-254890; $G_{q/11}$ signaling; analgesia; opioids; pain

INTRODUCTION

G protein-coupled receptors (GPCRs) constitute the largest family of cell surface receptors with immense roles in nearly all known physiological processes including nociception, cardiovascular function, and inflammation among many others (Pfleger et al., 2019; Salzer et al., 2019; Sun et al., 2012). Accordingly, GPCRs are frequently targeted by small molecule drugs for therapeutic benefits (Davenport et al., 2020; Hauser et al., 2017). However, the pleiotropic effects associated with their activation or inhibition also often lead to unwanted side effects (Brianso et al., 2011; Sriram et al., 2018). Many GPCR actions are mediated by heterotrimeric G proteins (Neves et al., 2002; Oldham et al., 2008). GPCRs activate G proteins by catalyzing their nucleotide exchange leading to the release of Gβγ subunits from Gα (Hollmann et al., 2005). Both active Gα-GTP and free Gβγ transduce signals by interacting with a range of downstream effector molecules to elicit a cellular response (Hubbard et al., 2006). There are 12 Gα subunits in mammals, grouped into 5 subfamilies ($Gα_{s/olf}$, $Gα_{i/o}$, $Gα_{q/11}$, $Gα_{12/13}$ and $Gα_{15}$) and characterized by unique properties and selectivity with which they regulate their effectors (Hilger et al., 2018; Masuho et al., 2015). Studies with knockout mice indicate that individual G protein channels selectively contribute to various aspects of GPCR signaling and physiological reactions controlled by them (Cha et al., 2019; van den Bos et al., 2020).

Most GPCRs can activate several different G proteins and signaling from different GPCRs also converge on the same set of G proteins (Marinissen et al., 2001). Furthermore, there is also significant evidence for both synergistic and opposing influence of different G proteins in regulating their effector molecules (Gupte et al., 2017; Oduori et al., 2020; Van Eps et al., 2018). Together, this points to the interplay between individual Gα as an important, yet not well understood, process in shaping GPCR signaling and in vivo actions of these receptors. Accordingly, pharmacological targeting of individual G proteins is emerging as an attractive strategy with therapeutic potential (Campbell et al., 2018).

One particularly prominent pharmacological area of need is the modulation of pain. GPCR signaling is heavily involved in this process with many receptors strategically positioned across both ascending and descending nociceptive circuits and noted involvement in regulating various pain states (Geppetti et al., 2015). A notable example is provided by the mu-opioid receptor (MOR) heavily targeted by opioid drugs to produce powerful analgesia (Gálvez et al., 2012). Notably, several other GPCR systems produce powerful analgesia (Stone et al., 2009). However, most of these also trigger unwanted side effects including, dependence, somatic, dysphoria prompting the search for alternative analgesic strategies (Volkow et al., 2016).

In contrast to largely anti-nociceptive effects associated with activation of $G_{i/o}$ receptors (Galeotti et al., 2002; Yudin et al., 2018), triggering G_q and G_s signaling generally leads to opposite outcomes, i.e. hyperalgesia, sensitization to pain, allodynia (Crain et al., 2000; Malin et al., 2010). Interestingly, increased expression of G_q and G_{11} proteins has been reported in animal models of pain (Belmadani et al., 2021; Saika et al., 2021). Genetic studies in mice indicate that loss of G_q and G_{11} results in reduced pain hypersensitivity in chronic pain states (Tappe-Theodor et al., 2012). Moreover, knockout of $G\alpha_{q/11}$ modulates properties of nociceptors, reduces basal pain sensitivity as well as pain sensitizing effects associated with activation of several $G\alpha_{q/11}$-coupled GPCRs (Wirotanseng et al., 2013). These observations suggest that suppressing $G_{q/11}$ may be a promising analgesic strategy.

Recently, related cyclic depsipeptides YM-254890 (YM) and FR-900359 (FR) were identified as potent and selective $G\alpha_q$ inhibitors. Their actions have been well characterized mechanistically (Nishimura et al., 2010) and they have been shown to have high chemical and metabolic stability (Schlegel et al., 2021). Their *in vivo* efficacy has been also established for cardiovascular effects (Meleka et al., 2019; Uemura et al., 2006a), yet they have not been evaluated for the effects in the nervous system. Here, we present the results of exploring the use of YM compound as an analgesic using acute pain models in mice. Using different routes of administration and nociceptive tests, we demonstrate in vivo anti-nociceptive efficacy of G_q inhibition in a stand-alone regime and in combination with opioids.

METHODS

Ethical statement

All studies were carried out in strict accordance with the recommendations in the Guide for the Care and Use of Laboratory Animals of the National Institute of Health. All procedures were approved by the Institutional Animal Care and Use Committee (IACUC) protocol (#16-032) at The Scripps Research Institute. Every effort was made to minimize the number of animals used in the following experiments. Animal studies are reported in compliance with the ARRIVE 2.0 (Percie du Sert et al., 2020) and the BJP (Lilley et al., 2020) guidelines.

Compliance with requirements for studies using animals

Because mice have been widely used in previous investigations for opioid related research (Jirkof, 2017), mice were used to allow comparisons of the current results with the previous literature. Mice were also appropriate because they have been widely used in translational pharmacological research on opioid analgesia and other neurological disorders. Consequently, to allow comparison between subcutaneous and intrathecal studies, mice were used for all the experiments. As sex-specific differences in thermal nociception have been reported following opioid administration, we compared both the routes of drug administration in male and female mice. Female mice were reported to be no more variable than male mice across diverse traits relevant to neuroscience studies (Becker et al., 2016). Thus, both male and female mice were used for all the experiments described in the current study.

Experimental animals

C57BL/6 mice (6-8 weeks old) of both sexes were used and were bred in the vivarium. Mice were housed in groups of 3-5 (unless otherwise stated) on a 12-h light-dark cycle (6:00 AM light cycle; 6:00 PM dark cycle) with food (Teklad Global 16% protein rodent diets; Envigo Inc., Wisconsin USA) and water available *ad libitum*. Animal groups were compiled to ensure minimization of factors (i.e., weight, sex, health). Mice were within 20-28 g in weight at start of all studies. All tested groups contained a control group and consisted of male and female mice. Males and females were tested on the same day but at different times so that they were not in the room at the same time. All the experiments were tested during the light cycle between 8:00 a.m. and 3:00 p.m. to avoid any long-term disruption of sleep cycles. Mice were transferred to the behavioral testing room at least 45 min before the first test to acclimatize.

Drug treatments

YM-254890 (henceforth referred to as YM) was purchased from AdipoGen® Life Sciences. The morphine used was sterile and free of preservatives (Morphine Sulphate, Sigma-Aldrich, St. Louis, MO, USA). For all in vivo studies, the vehicle used for YM compound is (0.05% DMSO in 5% dextrose solution) unless 0.9% saline is indicated as for morphine. To observe the systemic effects of YM administration, YM doses (0.1, 0.3, 0.5 and 1 mg/kg) was given subcutaneously. The dose of YM for subcutaneous injection was used from previous published studies (Meleka et al., 2019). The dose of morphine selected for subcutaneous administration (2.5, 5 and 10 mg/kg) is commonly used in mouse analgesia (Kest et al., 2002). For the combined administration of morphine and YM on thermal antinociception, YM was administered 10 min before the morphine. The latency of response was measured before injection of drugs (baseline latency response) and at different time intervals (post-treatment latency response) after drugs injection.

Intrathecal injections

Intrathecal (i.t.) administration was performed following the method described previously (Hylden et al., 1980; Li et al., 2019) with slight modifications. All intrathecal injections were performed using a 25 μl Hamilton syringe with a 30-gauge needle. The injection volume was 5 μl for each mouse. Data suggests that this is likely to be the upper limit that can be reliably injected into the mouse without any appreciable redistribution of the drugs through the cerebrospinal fluid to the basal cisterns of the brain (Rieselbach et al., 1962). Each solution was injected without injection cannulae. Intrathecal injections were made into the L5-L6 intervertebral space of unanesthetized mice. The flick of the tail was considered indicative of a successful i.t. administration.

Intracerebral injections

Intracerebroventricular (i.c.v.) administration was performed following the method described previously with slight modifications (Haley et al., 1957; Narita et al., 2003). On the day of the drug/vehicle injection or on the day of behavior test, the mouse was secured at the nape of the neck and head by the investigator's thumb and forefinger and head of the mouse was held against a V-shaped holder. A 27-gauge hypodermic needle attached with 25-μl

Hamilton microsyringe was inserted perpendicularly into the unilateral injection site into the hole with the depth of 3.5 mm. The injection volume was 4 μl.

Behavior assessment

Hot Plate test—Animals were tested for the assessment of antinociception and analgesic effects of morphine using hotplate set to 52.5 °C. The assay was performed as described previously (Bannon et al., 2007; Wang et al., 2019). Mice were place in a Plexiglass chamber (16" tall, 8" in diameter) on a ceramic plate heated to 52.5 °C and the timer started (Ugo Basile, Varese, Italy). Paw licking, paw flicking, and jumping were coded as a nociceptive response, upon which the timer was stopped or up to a maximum of 20 s (for YM or Vehicle) or 50 s (for morphine). Three trials were made with a 3 min intertrial interval. The mean paw-withdrawal latency from the three trials was used as the baseline latency. The analgesic effect of drug or vehicle was then determined by a single measurement of paw withdrawal or paw flicking or jumping latencies at respective time intervals. On the test day, mice were first tested for the baseline measurement (t=0, no drug/vehicle given), and the response latency was recorded. The drug (YM or vehicle or morphine) was given after few minutes and the nociceptive response was recorded at 10, 20, 30, 60, 90 and 120 min and up to the time until reached to baseline. For the combined administration effect of YM with morphine, YM was administered 10 min before the administration of morphine. Time (seconds) spent on hotplate was graphed as percent maximum possible effect (MPE). MPE (%) = (test latency - baseline latency/cut-off time – baseline latency x 100). Nociceptive responses were monitored on alternate days.

Tail Immersion test—Antinociception induced by YM, or evaluation of morphine's analgesic effects was determined by tail immersion test. The test was performed as previously described (Wang et al., 2019). Individual mice were transferred to experimentation room and restrained using a well-ventilated 50 ml tube with airholes. In order to minimize handling and to facilitate both the drug delivery and testing, each mouse was comfortably positioned in the plastic restrainer tubes with both fore paws and hind paws extending through holes at the bottom of the restrainer. All animals were habituated to restraint 1 hour/3 days prior to behavior test. After three days of training, mouse usually voluntarily entered the tube-shaped restrainer during the behavioral testing. No sign of distress was observed in these mice during restraint. Once the animal was immobilized (within 25-30 s), 2/3 of entire tail was dipped in water bath heated to 54 °C. Based on our preliminary experiments and reported by others (Bohn et al., 2002; Stone et al., 1997), the tail flick latency is required to be relatively short (2-3 s) for the test to remain valid. To achieve these latencies water bath temperature was varied and determined to be 54 °C. The tail flick latency was defined as the time from the onset of thermal heat to tail withdrawal. Three trials were made with a 3 min intertrial interval in between. The mean tail-flick latency from the three trials was used as the baseline latency. The analgesic effect of drug or vehicle was then determined by a single measurement of tail flick latencies at respective time intervals. A maximum cut-off was 10 s (for YM or vehicle) or 20 s (for morphine). The results were then expressed as a percent of the MPE using the equation described above. On the test day, mice were first tested for the baseline measurement (t=0, no drug/vehicle given), and the response latency was recorded. The drug (YM or vehicle or morphine) was

given after few minutes and the nociceptive response was recorded at 10, 20, 30, 60, 90 and 120 min and up to the time until reached to baseline. For the combined administration effect of YM with morphine, YM was administered 10 min before the administration of morphine.

Open field test—The open-field test was used to measure the locomotor activity in animals, where both baseline activity and drug-induced changes can be quantified (Prut et al., 2003). The distance travelled during the test period was recorded as the index of locomotor activity. Locomotor activity and position within the open field was measured for 2 h. The multiple unit open field maze consisted of four activity chambers. Each chamber was made from white high density and non-porous plastic and measured 50 x 50 x 38 cm^3. The mouse was placed individually in the centre of an open field arena with light bottom to contrast with animal color and the test started immediately. Light in the chamber was measured to be 40 lux. The arena was cleaned between each test using alcohol 70% to avoid interfering with the smell of the previously tested animal. The exploratory activity was analyzed within 2 h. Videos were analyzed using an EthoVision XT16 system (Noldus Information Technology, Wageningen, The Netherlands) considering two previously defined areas: a central and an outer arena.

Randomization and blinding

Randomization was best accomplished as follows. Animals were first assigned a group designation and weighed. Six different cohort of C57BL/6J animals were used for the four different behavioral testing as reported in systemic (2 cohorts for hot plate and tail immersion test), spinal (1 cohort), central (1 cohort) and open field test (2 cohorts for systemic and spinal administration) paradigms. For each cohort, total of 12 mice (6 male and 6 female) were divided into two different groups (6 animals: 3 males and 3 females per group). Then each mouse was assigned a temporary random number within that group. Then, the cages were randomized within the experimental group. All recordings were blinded prior to scoring. Experimental results that were not blinded were collected by program software. Program software was calibrated (~30 min before starting the experiment). No animals were excluded prior to and during studies since all were healthy.

Acutely dissociated DRG Preparation

Male or female mice between 1-2 months of age were used for acute DRG isolations. Dissociated DRG cultures were prepared as previously described (Perner et al., 2021). Briefly, DRG's were dissected from 1-2 month old mice in HBSS and digested with Collagenase A and Dispase II (Sigma-Aldrich) for 25 minutes at 37°, centrifuged at 200x *g* for 5 minutes, and washed with DMEM supplemented with 10% FBS, glutamate, sodium pyruvate, 1% penicillin, and 1% streptomycin. DRG were then triturated in Neurobasal A medium supplemented with 10% FBS, 1% penicillin, 1% streptomycin, 1% GlutaMax, 2% B27, 25ng/L NGF, and 2ng/L GDNF. After plating on laminin-coated coverslips, cells were incubated at 37°C overnight. Experiments were performed the day after dissection.

Whole cell patch-clamp recordings

Nociceptors were identified by physiologic classification protocols (Petruska et al., 2000) summarized in Supplementary Figure S5, and further by responsivity to morphine. Each

experimental group consisted of 12-18 DRG recordings from 3 animals, 1-2 of which were female. Hyperpolarization-activated current (I_h) and kinetics of resulting transient currents were determined by stepping membrane potential from −60 mV to −110 mV for 500 ms in 10 mV increments (Supplementary Figure S4A). Outward currents were identified by first preconditioning membrane potential at −100mV for 500ms, then stepping from −60 mV to 40 mV in 20mV increments for 200ms (Supplementary Figure S4D). Inward current dynamics were determined by preconditioning at −80 mV, then stepping from −60 mV to 40 mV in 10 mV increments (Supplementary Figure S4G). A 6-second, 0-2 nA continuous ramp stimulation protocol was used to determine rheobase. Membrane capacitance (C_m), series resistance (Rs) and input resistance (Ri) were tested with a hyperpolarizing 10 mV pulse of 10ms duration initially and at a 30 second interval throughout the recording period. Cells were recorded only if initial series resistance 20MΩ and excluded if Rs varied >20% while recording. Offline analysis identified clustering of a population N = 30 with uniform morphine responsivity that was selected for further analysis, with basal parameters ± SEM; C_m = 27.31 ± 4.72 pF, Ri = 492 ± 19.29 MΩ, I_h = 7.10 ± 2.45 pA/pF, I_A tau = 8.39 ± 0.41ms, and action potential tau = 1.22 ± 0.08ms. K^+ internal was used for all recordings, containing in mM: 6 NaCl, 4 NaOH, 130 K-gluconate, 11 EGTA, 1 $CaCl_2$, 1 $MgCl_2$, 10 HEPES, 2 Na_2ATP, and 0.2 Na_2GTP, adjusted to pH 7.3-7.4 with HCl. External aCSF contained in mM: 125 NaCl, 3 KCl, 1.2 KH_2PO_4, 1.2 $MgSO_4$, 25 $NaHCO_3$, 2 $CaCl_2$, 10 dextrose, adjusted to pH 7.3-7.4 with HCl.

Data collection and statistical analysis

Sample sizes appropriate for each type of experiment were estimated based on pilot studies and were calculated based on the equation (Eng, 2003): CI_{95} = 1.96/ n, where *CI* stands for the confidence interval, 1.96 is the corresponding tabulated value for CI_{95}, *s* is the standard deviation of the mean and *n* is the sample size. When experiments are novel, it is difficult to perform a priori sample size calculations (Curtis et al., 2018) because the effect size and variance are unknown. Therefore, for animal experiments, estimates of the expected variance and effect size from previous experiments using similar methods were used to estimate appropriate sample sizes a priori through statistical power calculations. Data are presented as mean ± SEM. A D'Agostino-Pearson test and Shapiro-Wilk normality tests were applied to evaluate data normality and homogeneity. Parametric statistics for normally distributed variables included unpaired t-test and two-way ANOVA. In addition, group differences using two factors or independent variables were evaluated by two-way ANOVA. Bonferroni 's *post-hoc* for multiple comparisons was applied when the main effects of factor were significant in the ANOVA analysis. A non-parametric test (Spearman rank, *R*) was used to check correlations when one of the variables was not normally distributed. Kruskal-Wallis non-parametric test followed by Dunn's multiple comparison test was applied for the data that was not normally distributed. For the open field test, data recorded by Etho Vision software were exported and tabulated in excel. Thereafter, statistical analysis of these data was carried out using GraphPad prism software. No animals were excluded from the study, and the data were monitored for statistically outliers. For electrophysiological data, measurements were performed with ClampFit version 10.5 (Molecular Devices, San Jose, California, USA). All the statistical analysis was performed using GraphPad Prism version 9.0.0 for Windows (GraphPad Software, San Diego, California, USA). The post hoc tests

were only applied when ANOVA results were significant. A p value less than 0.05 ($p < 0.05$), was considered statistically significant.

Compliance with design and statistical analysis requirements

The manuscript complies with the design and statistical analysis requirements of the British Journal of Pharmacology (Curtis et al., 2015) and its update (Curtis et al., 2018).

Nomenclature of Targets and Ligands

Key protein targets and ligands in this article are hyperlinked to corresponding entries in http://www.guidetopharmacology.org, the common portal for data from IUPHAR/BPS Guide to PHARMACOLOGY (Harding et al., 2018), and are permanently archived in the Concise Guide to PHARMACOLOGY 2019/20 (Alexander et al., 2021).

RESULTS

Effects of YM administration on central nociception and locomotion.

We started by evaluating the effects of YM on pain responses of mice in the hot plate test by performing the dose response studies administering the drug systemically via subcutaneous injections. A concentration range of 0.1 - 1 mg/kg that we explored was reported to be safe for systemic administration (Meleka et al., 2019). We found that treatment with YM at higher doses (0.5 and 1.0 mg/kg) produced increase in paw withdrawal latencies reaching maximal analgesic response at 30 min (unpaired t-test, $P < 0.05$) after injection (Figure 1A and Supplementary Figures S1A). We observed no significant effect of YM at lower doses (0.1 and 0.3 mg/kg) (Figure 1A and Supplementary Figures S1A). To confirm that YM directly affects central nervous system to produce analgesic effects, the drug was delivered directly into the brain. Indeed, we observed a dose-dependent increase in both the extent and duration of analgesia upon YM administration (Supplementary Figure S2).

Next, we evaluated the effect of YM treatment on opioid induced analgesia. Administration of subthreshold dose of YM (0.25 mg/kg) significantly potentiated anti-nociceptive effects in the hot plate test (Figure 1B and Supplementary Figure S1B). Increasing the dose (YM 0.5 mg/kg) led to further enhancement of opioid analgesia (Figure 1B and Supplementary Figure S1B). Interestingly, while YM treatment increased the maximal degree of the effect, it had no effect on either the onset timing or duration of the opioid analgesia with all the animals reaching maximal latencies in ~30 min and recovering to the baseline nociceptive thresholds in ~ 3 hours.

To evaluate effects of YM treatment on locomotion behavior, mice were tested in the open field test. We injected YM compounds at the doses that produce the most significant analgesic effects both alone and in combination with morphine. Analysis of the results indicated that while morphine alone produced well known locomotor sensitizing effect, co-treatment with the YM completely suppressed these effects and resulted in substantial decrease in locomotion comparable to the levels seen with the YM treatment alone (Figure 1C).

Effects of systemic Gα$_{q/11}$ inhibition on spinal analgesia.

Because changes in locomotor activity can confound the interpretation of the hot plate test which relies on complex body movements, we next used the tail flick test which relies on spinal reflexes to assess nociception in mice. We found that YM induced significant anti-nociceptive response at the highest dose of 1 mg/kg (Figure 2A and Supplementary Figure S3A). However, no significant difference in nociception response was observed on lower doses (Figure 2A and Supplementary Figures S3A).

Next, we evaluated the effect of YM treatment at subthreshold doses of morphine analgesia using the same tail immersion test (Figure 2B). We observed significant enhancement of anti-nociceptive effects of morphine at 0.5 mg/kg dose of YM (Figure 2B and Supplementary Figure S3B). Reducing the dose to 0.25 mg/kg eliminated this effect (Figure 2B and Supplementary Figure S3B). In summary, these results indicate that when administered systemically YM has analgesic properties which are however confounded by effects on locomotor behavior.

Analgesic properties of intrathecal YM treatment and its synergy with opioids.

To avoid the side-effects associated with systemic YM administration, we explored spinal intrathecal delivery, a route routinely used in clinical practice for mitigating unwanted effects especially in the context of opioid treatment (Fairbanks, 2003). When injected intrathecally, YM showed significant anti-nociceptive properties in the tail immersion test at doses above 1.5 nmol per injection (Figure 3A and Supplementary Figure S4A). The magnitude of the effect did not change upon increasing the dose to 4.5 nmol suggesting the ceiling effect. The duration of the effect did not differ between the two maximally effective doses (3.0 and 4.5 nmol) with the animals returning to baseline nociception in about two hours (Figure 3A and Supplementary Figure S4A).

As before, we next tested the effects of intrathecal YM administration on systemic morphine analgesia in the tail immersion test. We observed that the lowest subthreshold dose of 0.5 nmol already significantly enhanced the anti-nociceptive effects of morphine (Figure 3B and Supplementary Figure S4B). This effect was increased dose dependently until maxing out at the cut-off value for the test (Supplementary Figure S4B). At each of the dose both the maximal extent and duration of the analgesic effects of morphine were increased. Because inhibition of motor activity was a significant confound of the YM-induced analgesia upon systemic administration, we further monitored its effects on animal locomotion following intrathecal delivery. As expected from local delivery method, we found no significant changes in motor activity induced by YM either when administered alone or in combination with morphine (Figure 3C). Together, these results indicate effectiveness of YM as analgesic at the level of spinal cord and its substantial synergy with opioid induced analgesia.

Gα$_{q/11}$ inhibition suppresses activity of DRG nociceptors and augments their responsiveness to opioid inhibition.

To obtain insights into the mechanisms by which inhibition of G$_{q/11}$ produces analgesic effects and enhances morphine action we examined the impact of YM on electrophysiological properties of dorsal root ganglia (DRG) nociceptors in the peripheral

nervous system. These neurons play a crucial role in nociception and express the direct target of opioid analgesics – MOR (Rau et al., 2005; Ruda, 1986).

DRG nociceptors were identified by multiple electrophysiological characteristics (Supplementary Figure S5) including presence of hyperpolarization activated current, A-type current inactivation rate, inward current dynamics and responsiveness to morphine. The effectiveness of YM as a $G_{q/11}$ antagonist in this population was verified by its ability to inhibit the effects of <u>substance P</u> which mediates its effects via canonical $G_{q/11}$ -coupled pathway (Supplementary Figure S6). Consistent with prior observations (Mizuta et al., 2012; Womack et al., 1995), application of morphine substantially decreased excitability of these DRG neurons as evidenced by significant increase in rheobase when using ramp stimulation protocol (Figure 4A-B). Treatment with YM alone also caused significant decrease in the excitability of DRG nociceptors (Figure 4A-B). The magnitude of this effect was smaller as compared to morphine consistent with the lower analgesic efficacy of YM relative to morphine observed in behavioral studies. A similar interaction was observed with resting input resistance (Figure 4C).

To better understand these effects, we further studied AP dynamics with a voltage-step protocol (Supplementary Figure S5G-I). Again, application of either YM or morphine moderately reduced AP amplitude to approximately similar extent (Figure 4C-D). However, co-application of YM and morphine largely prevented evoked AP responses (Figure 5A-B). This synergistic interaction was also apparent in the modulation of rapidly inactivating A-type potassium currents (I_A) tested with voltage-step protocol 2 (Supplementary Figure S5D-F). Both YM and morphine significantly inhibited I_A, while their coadministration nearly eliminated I_A. These physiological effects demonstrate that YM and morphine interact synergistically to reduce nociceptor excitability as a mechanism for producing analgesic effects.

DISCUSSION

In this study we demonstrate that in vivo pharmacological inhibition of $G_{q/11}$ induces antinociception in a mouse model of thermal pain. When administered intrathecally to healthy adult mice, YM produced analgesia in a dose-dependent manner without noticeable side effects. The efficacy of this analgesia was moderate and reached the ceiling around 30% of the maximal antinociceptive effect that could be recorded in the test we used. However, local YM administration produced marked enhancement of analgesic effect of morphine. Intrathecal YM at the highest dose we used essentially maxed out otherwise low pain suppressant effect of low dose of morphine producing extremely long lasting and potent analgesia. These observations suggest that while tonically active $G\alpha_{q/11}$ signalling contributes to setting nociceptive thresholds, its major role is likely in intersecting with the receptor signaling pathways, e.g. MOR involved in analgesia.

The involvement of $G\alpha_{q/11}$ signaling in pain was suggested by earlier genetic studies in mice targeting the $G_{q/11}$ pathway and the interventions at the level of G_q-coupled GPCRs and downstream $G_{q/11}$ effectors also showed modulation of pain responses (Tappe-Theodor et al., 2012; Wirotanseng et al., 2013). To the best of our knowledge the present study is the

first to explore direct pharmacological blockade of $G\alpha_{q/11}$ in the context of pain and nervous system actions. This was made possible by recent development of compounds targeting $G\alpha_{q/11}$- YM and FR. The YM compound used in this study is a selective and efficacious G_q inhibitor isolated from chromobacterium species (Taniguchi et al., 2003). Although specificity of YM across different $G\alpha$ subunits was questioned (Peng et al., 2021), recent thorough investigation unequivocally established its selectivity towards $G\alpha_q$ and $G\alpha_{11}$ (Patt et al., 2021).

Previously, the therapeutic potential of YM was demonstrated for promoting antithrombotic and vasodilatory effects in mice, rats, and monkeys (Kawasaki et al., 2003; Kawasaki et al., 2005; Uemura et al., 2006a; Uemura et al., 2006b). In these studies, the $G_{q/11}$ inhibitor YM (1-30 μg/kg) was administered as bolus injection directly into the blood stream, and resulted in substantial lowering of the systemic blood pressure. Very few studies examined performed systemic YM administration, where effects were observed with dosing ranging between 0.15 mg/kg and 7.5 mg/kg (Hitchman et al., 2021; Roszko et al., 2017). This generally agrees with the range of 0.1 – 1 mg/kg of YM that we delivered subcutaneously to observe analgesic effects. Intrathecal and intracerebroventricular routes were explored in this study for the first time. We think our observations that YM inhibited locomotor activity of mice is related to its depressant effects on cardiovascular function which likely limit the utility of the systemic YM administration as an analgesic. We showed that these limitations could be bypassed by local administration of YM into the spinal cord which produced efficacious analgesia without locomotor/cardiovascular side effects. Indeed, spinal delivery of YM may be achievable in humans, because intrathecal and epidural injections presents a clinically viable route for the delivery of analgesics (Bottros et al., 2014) and because the spinal cord is the first relay site in the transmission of nociceptive information in the central nervous system (Zhuo et al., 2011).

A particularly intriguing observation of our study is an ability of YM to markedly enhance efficacy of opioid analgesics. This could allow lowering the dose of opioids administered which will likely be beneficial to mitigating side-effects associated with opioid therapies. Our mechanistic studies indicate that major site of this interaction occurs at the level of primary nociceptive neurons in the DRG located in the peripheral nervous system. Electrophysiological recordings revealed that while both YM and morphine can supress excitability of DRG nociceptors, their combinatorial application has a synergistic effect completely supressing their firing thereby blocking reception of noxious stimuli.

Current therapeutically useful opioids such as morphine produce their analgesic and respiratory depression side-effects through activation of μ-opioid receptor (MOR) (Matthes et al., 1996). The MOR is a GPCR that signals through activation of $G_{i/o}$ proteins and also via β-arrestin recruitment (Williams et al., 2013). Differential engagement of effectors downstream from MOR activation, so called biased signaling or functional selectivity, is thought differentially contribute to various effects associated with MOR engagement including its main therapeutic action: analgesia and unwanted collateral effects such as respiratory depression, constipation and euphoria (DeWire et al., 2013; Manglik et al., 2016). The main focus in the field has been largely on exploring G protein vs β-arrestin engagement in the efforts to explain functional selectivity of MOR and exploit it

therapeutically for dissociating opioid analgesia from the side-effects (Bateman et al., 2021; Pineyro et al., 2021). However, recent evidence questioned the utility of this concept (Gillis et al., 2020) suggesting that other signaling mechanisms may be at play in routing MOR signals. One attractive area with significant potential for explaining how routing of MOR signals can be biased is its signaling cross-talk with other receptor-systems that converge on common effectors to allow differential programming of cellular responses. Several signaling systems impacting processing of MOR signals and in vivo opioid actions have been described (Gibula-Tarlowska et al., 2020). Interestingly, studying one of these systems we found that blockade of $G_{q/11}$-coupled orphan receptor GPR139 exerted augmentation of opioid signaling via MOR and dissociated analgesia from withdrawal at the behavioral level (Wang et al., 2019). These findings are in line with other elements in the G_q pathway counteracting opioid effects initiated by MOR (Javed et al., 2004; Mathews et al., 2008). Thus, we think that our observations with the YM compound enhancing opioid analgesia falls under the same overall theme as these and is likely explained by lifting the G_q effects on downstream effectors such as adenylyl cyclase (AC) and ion channels (Halls et al., 2017; Stoveken et al., 2020) that oppose $G_{i/o}$ signaling initiated by MOR. Alternatively, blockade of the $G_{q/11}$ may diminish desensitizing regulation of MOR by PLCβ-PKC axis (Bailey et al., 2009; Xie et al., 1999), a major effector system of $G_{q/11}$ proteins. The exact mechanisms and intersecting points of such cross-talk are of interest to determine and should be the focus of the future studies.

Our study also has some limitations that will need to be addressed in future. Our experiments have been restricted to acute pain and nociceptor physiology in a mouse model. Although we could exclude locomotor and acute cardiovascular side effects of YM, future work will need to investigate longer-term YM effects on other organ systems and during chronic application and translate these observations to other species. Examining the efficacy of YM and other $G_{q/11}$ inhibitors in chronic and neuropathic pain models both alone and in combination with opioids also seems warranted. Nevertheless, we believe that the current study demonstrates the utility of pharmacological inhibition of G_q signaling as an analgesic strategy.

CONCLUSION

Our findings provide the evidence that pharmacological inhibition of $G_{q/11}$ is anti-nociceptive and enhances opioid analgesia. We hope these observations will spur further research in potential application of $G_{q/11}$ as a pain management strategy.

Supplementary Material

Refer to Web version on PubMed Central for supplementary material.

Acknowledgments

Data Availability

All data is presented in the manuscript or supplementary information.

List of Abbreviations:

AC	Adenylyl cyclase
CSF	Cerebrospinal fluid
DMEM	Dulbecco's modified Eagle's medium
DRG	Dorsal Root Ganglion
FBS	Fetal bovine serum
GDNF	Glial cell line-derived neurotrophic factor
GPCR	G protein-coupled receptor
HBSS	Hank's buffered salt solution
HEPES	N-[2-hydroxyethyl]piperazine-N'[2-ethanesulphonic acid]
i.t.	intrathecal
MOR	μ-opioid receptor
NGF	Nerve growth factor
PLCβ	Phospholipase C Beta
s.c.	subcutaneous

REFEERNCES

Alexander SPH, Christopoulos A, Davenport AP, Kelly E, Mathie A, Peters JA, et al. (2021). THE CONCISE GUIDE TO PHARMACOLOGY 2021/22: G protein-coupled receptors. British Journal of Pharmacology 178: S27–S156. [PubMed: 34529832]

Bailey CP, Llorente J, Gabra BH, Smith FL, Dewey WL, Kelly E, et al. (2009). Role of protein kinase C and mu-opioid receptor (MOPr) desensitization in tolerance to morphine in rat locus coeruleus neurons. Eur J Neurosci 29: 307–318. [PubMed: 19200236]

Bannon AW, & Malmberg AB (2007). Models of nociception: hot-plate, tail-flick, and formalin tests in rodents. Curr Protoc Neurosci Chapter 8: Unit 8 9.

Bateman JT, & Levitt ES (2021). Evaluation of G protein bias and β-arrestin 2 signaling in opioid-induced respiratory depression. American Journal of Physiology-Cell Physiology 321: C681–C683. [PubMed: 34469203]

Becker JB, Prendergast BJ, & Liang JW (2016). Female rats are not more variable than male rats: a meta-analysis of neuroscience studies. Biol Sex Differ 7: 34. [PubMed: 27468347]

Belmadani A, Jayaraj ND, George DS, Ren D, Rathwell C, Miller RJ, et al. (2021). Activation of Keratinocyte Gq-linked G-Protein Coupled Receptors Regulates Degeneration of Cutaneous Nerves. The Journal of Pain 22: 581.

Bohn LM, Lefkowitz RJ, & Caron MG (2002). Differential mechanisms of morphine antinociceptive tolerance revealed in (beta)arrestin-2 knock-out mice. J Neurosci 22: 10494–10500. [PubMed: 12451149]

Bottros MM, & Christo PJ (2014). Current perspectives on intrathecal drug delivery. J Pain Res 7: 615–626. [PubMed: 25395870]

Brianso F, Carrascosa MC, Oprea TI, & Mestres J (2011). Cross-pharmacology analysis of G protein-coupled receptors. Curr Top Med Chem 11: 1956–1963. [PubMed: 21851335]

Campbell AP, & Smrcka AV (2018). Targeting G protein-coupled receptor signalling by blocking G proteins. Nat Rev Drug Discov 17: 789–803. [PubMed: 30262890]

Cha HL, Choi J-M, Oh H-H, Bashyal N, Kim S-S, Birnbaumer L, et al. (2019). Deletion of the α subunit of the heterotrimeric Go protein impairs cerebellar cortical development in mice. Molecular Brain 12: 57. [PubMed: 31221179]

Crain SM, & Shen KF (2000). Antagonists of excitatory opioid receptor functions enhance morphine's analgesic potency and attenuate opioid tolerance/dependence liability. Pain 84: 121–131. [PubMed: 10666516]

Curtis MJ, Alexander S, Cirino G, Docherty JR, George CH, Giembycz MA, et al. (2018). Experimental design and analysis and their reporting II: updated and simplified guidance for authors and peer reviewers. Br J Pharmacol 175: 987–993. [PubMed: 29520785]

Curtis MJ, Bond RA, Spina D, Ahluwalia A, Alexander SP, Giembycz MA, et al. (2015). Experimental design and analysis and their reporting: new guidance for publication in BJP. Br J Pharmacol 172: 3461–3471. [PubMed: 26114403]

Davenport AP, Scully CCG, de Graaf C, Brown AJH, & Maguire JJ (2020). Advances in therapeutic peptides targeting G protein-coupled receptors. Nature Reviews Drug Discovery 19: 389–413. [PubMed: 32494050]

DeWire SM, Yamashita DS, Rominger DH, Liu G, Cowan CL, Graczyk TM, et al. (2013). A G Protein-Biased Ligand at the μ-Opioid Receptor Is Potently Analgesic with Reduced Gastrointestinal and Respiratory Dysfunction Compared with Morphine. Journal of Pharmacology and Experimental Therapeutics 344: 708–717. [PubMed: 23300227]

Eng J (2003). Sample size estimation: how many individuals should be studied? Radiology 227: 309–313. [PubMed: 12732691]

Fairbanks CA (2003). Spinal delivery of analgesics in experimental models of pain and analgesia. Adv Drug Deliv Rev 55: 1007–1041. [PubMed: 12935942]

Galeotti N, Ghelardini C, & Bartolini A (2002). Antihistamine antinociception is mediated by Gi-protein activation. Neuroscience 109: 811–818. [PubMed: 11927163]

Gálvez R, & Pérez C (2012). Is morphine still the best reference opioid? Pain Manag 2: 33–45. [PubMed: 24654616]

Geppetti P, Veldhuis Nicholas A, Lieu T, & Bunnett Nigel W (2015). G Protein-Coupled Receptors: Dynamic Machines for Signaling Pain and Itch. Neuron 88: 635–649. [PubMed: 26590341]

Gibula-Tarlowska E, & Kotlinska JH (2020). Crosstalk between Opioid and Anti-Opioid Systems: An Overview and Its Possible Therapeutic Significance. Biomolecules 10.

Gillis A, Kliewer A, Kelly E, Henderson G, Christie MJ, Schulz S, et al. (2020). Critical Assessment of G Protein-Biased Agonism at the μ-Opioid Receptor. Trends Pharmacol Sci 41: 947–959. [PubMed: 33097283]

Gupte TM, Malik RU, Sommese RF, Ritt M, & Sivaramakrishnan S (2017). Priming GPCR signaling through the synergistic effect of two G proteins. Proceedings of the National Academy of Sciences 114: 3756–3761.

Haley TJ, & McCormick WG (1957). Pharmacological effects produced by intracerebral injection of drugs in the conscious mouse. Br J Pharmacol Chemother 12: 12–15. [PubMed: 13413144]

Halls ML, & Cooper DMF (2017). Adenylyl cyclase signalling complexes – Pharmacological challenges and opportunities. Pharmacology & Therapeutics 172: 171–180. [PubMed: 28132906]

Harding SD, Sharman JL, Faccenda E, Southan C, Pawson AJ, Ireland S, et al. (2018). The IUPHAR/BPS Guide to PHARMACOLOGY in 2018: updates and expansion to encompass the new guide to IMMUNOPHARMACOLOGY. Nucleic Acids Res 46: D1091–D1106. [PubMed: 29149325]

Hauser AS, Attwood MM, Rask-Andersen M, Schiöth HB, & Gloriam DE (2017). Trends in GPCR drug discovery: new agents, targets and indications. Nat Rev Drug Discov 16: 829–842. [PubMed: 29075003]

Hilger D, Masureel M, & Kobilka BK (2018). Structure and dynamics of GPCR signaling complexes. Nat Struct Mol Biol 25: 4–12. [PubMed: 29323277]

Hitchman TD, Bayshtok G, Ceraudo E, Moore AR, Lee C, Jia R, et al. (2021). Combined Inhibition of Gα(q) and MEK Enhances Therapeutic Efficacy in Uveal Melanoma. Clin Cancer Res 27: 1476–1490. [PubMed: 33229459]

Hollmann Markus W, Strumper D, Herroeder S, Durieux Marcel E, & Warltier David C (2005). Receptors, G Proteins, and Their Interactions. Anesthesiology 103: 1066–1078. [PubMed: 16249682]

Hubbard KB, & Hepler JR (2006). Cell signalling diversity of the Gqalpha family of heterotrimeric G proteins. Cell Signal 18: 135–150. [PubMed: 16182515]

Hylden JL, & Wilcox GL (1980). Intrathecal morphine in mice: a new technique. Eur J Pharmacol 67: 313–316. [PubMed: 6893963]

Javed RR, Dewey WL, Smith PA, & Smith FL (2004). PKC and PKA inhibitors reverse tolerance to morphine-induced hypothermia and supraspinal analgesia in mice. Eur J Pharmacol 492: 149–157. [PubMed: 15178359]

Jirkof P (2017). Side effects of pain and analgesia in animal experimentation. Lab Anim (NY) 46: 123–128. [PubMed: 28328895]

Kawasaki T, Taniguchi M, Moritani Y, Hayashi K, Saito T, Takasaki J, et al. (2003). Antithrombotic and thrombolytic efficacy of YM-254890, a G q/11 inhibitor, in a rat model of arterial thrombosis. Thromb Haemost 90: 406–413. [PubMed: 12958608]

Kawasaki T, Taniguchi M, Moritani Y, Uemura T, Shigenaga T, Takamatsu H, et al. (2005). Pharmacological properties of YM-254890, a specific G(alpha)q/11 inhibitor, on thrombosis and neointima formation in mice. Thromb Haemost 94: 184–192. [PubMed: 16113802]

Kest B, Hopkins E, Palmese CA, Adler M, & Mogil JS (2002). Genetic variation in morphine analgesic tolerance: A survey of 11 inbred mouse strains. Pharmacology Biochemistry and Behavior 73: 821–828. [PubMed: 12213527]

Li D, Li Y, Tian Y, Xu Z, & Guo Y (2019). Direct Intrathecal Injection of Recombinant Adeno-associated Viruses in Adult Mice. J Vis Exp.

Lilley E, Stanford SC, Kendall DE, Alexander SPH, Cirino G, Docherty JR, et al. (2020). ARRIVE 2.0 and the British Journal of Pharmacology: Updated guidance for 2020. Br J Pharmacol 177: 3611–3616. [PubMed: 32662875]

Malin SA, & Molliver DC (2010). Gi- and Gq-coupled ADP (P2Y) receptors act in opposition to modulate nociceptive signaling and inflammatory pain behavior. Mol Pain 6: 21. [PubMed: 20398327]

Manglik A, Lin H, Aryal DK, McCorvy JD, Dengler D, Corder G, et al. (2016). Structure-based discovery of opioid analgesics with reduced side effects. Nature 537: 185–190. [PubMed: 27533032]

Marinissen MJ, & Gutkind JS (2001). G-protein-coupled receptors and signaling networks: emerging paradigms. Trends Pharmacol Sci 22: 368–376. [PubMed: 11431032]

Masuho I, Ostrovskaya O, Kramer GM, Jones CD, Xie K, & Martemyanov KA (2015). Distinct profiles of functional discrimination among G proteins determine the actions of G protein-coupled receptors. Sci Signal 8: ra123. [PubMed: 26628681]

Mathews JL, Smrcka AV, & Bidlack JM (2008). A novel Gbetagamma-subunit inhibitor selectively modulates mu-opioid-dependent antinociception and attenuates acute morphine-induced antinociceptive tolerance and dependence. J Neurosci 28: 12183–12189. [PubMed: 19020012]

Matthes HW, Maldonado R, Simonin F, Valverde O, Slowe S, Kitchen I, et al. (1996). Loss of morphine-induced analgesia, reward effect and withdrawal symptoms in mice lacking the mu-opioid-receptor gene. Nature 383: 819–823. [PubMed: 8893006]

Meleka MM, Edwards AJ, Xia J, Dahlen SA, Mohanty I, Medcalf M, et al. (2019). Anti-hypertensive mechanisms of cyclic depsipeptide inhibitor ligands for Gq/11 class G proteins. Pharmacol Res 141: 264–275. [PubMed: 30634050]

Mizuta K, Fujita T, & Kumamoto E (2012). Inhibition by morphine and its analogs of action potentials in adult rat dorsal root ganglion neurons. J Neurosci Res 90: 1830–1841. [PubMed: 22488082]

Narita M, Imai S, Ozaki S, Suzuki M, Narita M, & Suzuki T (2003). Reduced expression of a novel mu-opioid receptor (MOR) subtype MOR-1B in CXBK mice: implications of MOR-1B in the expression of MOR-mediated responses. Eur J Neurosci 18: 3193–3198. [PubMed: 14686893]

Neves SR, Ram PT, & Iyengar R (2002). G Protein Pathways. Science 296: 1636–1639. [PubMed: 12040175]

Nishimura A, Kitano K, Takasaki J, Taniguchi M, Mizuno N, Tago K, et al. (2010). Structural basis for the specific inhibition of heterotrimeric G_q protein by a small molecule. Proceedings of the National Academy of Sciences 107: 13666–13671.

Oduori OS, Murao N, Shimomura K, Takahashi H, Zhang Q, Dou H, et al. (2020). Gs/Gq signaling switch in β cells defines incretin effectiveness in diabetes. The Journal of Clinical Investigation 130: 6639–6655. [PubMed: 33196462]

Oldham WM, & Hamm HE (2008). Heterotrimeric G protein activation by G-protein-coupled receptors. Nat Rev Mol Cell Biol 9: 60–71. [PubMed: 18043707]

Patt J, Alenfelder J, Pfeil EM, Voss JH, Merten N, Eryilmaz F, et al. (2021). An experimental strategy to probe Gq contribution to signal transduction in living cells. J Biol Chem 296: 100472. [PubMed: 33639168]

Peng Q, Alqahtani S, Nasrullah MZA, & Shen J (2021). Functional evidence for biased inhibition of G protein signaling by YM-254890 in human coronary artery endothelial cells. Eur J Pharmacol 891: 173706. [PubMed: 33152337]

Percie du Sert N, Hurst V, Ahluwalia A, Alam S, Avey MT, Baker M, et al. (2020). The ARRIVE guidelines 2.0: Updated guidelines for reporting animal research. PLoS Biol 18: e3000410. [PubMed: 32663219]

Perner C, & Sokol CL (2021). Protocol for dissection and culture of murine dorsal root ganglia neurons to study neuropeptide release. STAR Protoc 2: 100333. [PubMed: 33615276]

Petruska JC, Napaporn J, Johnson RD, Gu JG, & Cooper BY (2000). Subclassified acutely dissociated cells of rat DRG: histochemistry and patterns of capsaicin-, proton-, and ATP-activated currents. J Neurophysiol 84: 2365–2379. [PubMed: 11067979]

Pfleger J, Gresham K, & Koch WJ (2019). G protein-coupled receptor kinases as therapeutic targets in the heart. Nature Reviews Cardiology 16: 612–622. [PubMed: 31186538]

Pineyro G, & Nagi K (2021). Signaling diversity of mu- and delta- opioid receptor ligands: Re-evaluating the benefits of β-arrestin/G protein signaling bias. Cellular Signalling 80: 109906. [PubMed: 33383156]

Prut L, & Belzung C (2003). The open field as a paradigm to measure the effects of drugs on anxiety-like behaviors: a review. Eur J Pharmacol 463: 3–33. [PubMed: 12600700]

Rau KK, Caudle RM, Cooper BY, & Johnson RD (2005). Diverse immunocytochemical expression of opioid receptors in electrophysiologically defined cells of rat dorsal root ganglia. Journal of Chemical Neuroanatomy 29: 255–264. [PubMed: 15927787]

Rieselbach RE, Chiro GD, Freireich EJ, & Rall DP (1962). Subarachnoid Distribution of Drugs after Lumbar Injection. New England Journal of Medicine 267: 1273–1278. [PubMed: 13973811]

Roszko KL, Bi R, Gorvin CM, Bräuner-Osborne H, Xiong XF, Inoue A, et al. (2017). Knockin mouse with mutant Gα(11) mimics human inherited hypocalcemia and is rescued by pharmacologic inhibitors. JCI Insight 2: e91079. [PubMed: 28194446]

Ruda MA (1986). The Pattern and Place of Nociceptive Modulation in the Dorsal Horn. In Spinal Afferent Processing. ed Yaksh TL. Springer US: Boston, MA, pp 141–164.

Saika F, Matsuzaki S, Kishioka S, & Kiguchi N (2021). Chemogenetic Activation of CX3CR1-Expressing Spinal Microglia Using Gq-DREADD Elicits Mechanical Allodynia in Male Mice. Cells 10.

Salzer I, Ray S, Schicker K, & Boehm S (2019). Nociceptor Signalling through ion Channel Regulation via GPCRs. Int J Mol Sci 20.

Schlegel JG, Tahoun M, Seidinger A, Voss JH, Kuschak M, Kehraus S, et al. (2021). Macrocyclic Gq Protein Inhibitors FR900359 and/or YM-254890–Fit for Translation? ACS Pharmacology & Translational Science 4: 888–897. [PubMed: 33860209]

Sriram K, & Insel PA (2018). G Protein-Coupled Receptors as Targets for Approved Drugs: How Many Targets and How Many Drugs? Mol Pharmacol 93: 251–258. [PubMed: 29298813]

Stone LS, MacMillan LB, Kitto KF, Limbird LE, & Wilcox GL (1997). The alpha2a adrenergic receptor subtype mediates spinal analgesia evoked by alpha2 agonists and is necessary for spinal adrenergic-opioid synergy. J Neurosci 17: 7157–7165. [PubMed: 9278550]

Stone LS, & Molliver DC (2009). In search of analgesia: emerging roles of GPCRs in pain. Mol Interv 9: 234–251. [PubMed: 19828831]

Stoveken HM, Zucca S, Masuho I, Grill B, & Martemyanov KA (2020). The orphan receptor GPR139 signals via $G_{q/11}$ to oppose opioid effects. Journal of Biological Chemistry 295: 10822–10830. [PubMed: 32576659]

Sun L, & Ye RD (2012). Role of G protein-coupled receptors in inflammation. Acta Pharmacologica Sinica 33: 342–350. [PubMed: 22367283]

Taniguchi M, Nagai K, Arao N, Kawasaki T, Saito T, Moritani Y, et al. (2003). YM-254890, a novel platelet aggregation inhibitor produced by Chromobacterium sp. QS3666. J Antibiot (Tokyo) 56: 358–363. [PubMed: 12817809]

Tappe-Theodor A, Constantin CE, Tegeder I, Lechner SG, Langeslag M, Lepcynzsky P, et al. (2012). Gα(q/11) signaling tonically modulates nociceptor function and contributes to activity-dependent sensitization. Pain 153: 184–196. [PubMed: 22071319]

Uemura T, Kawasaki T, Taniguchi M, Moritani Y, Hayashi K, Saito T, et al. (2006a). Biological properties of a specific Galpha q/11 inhibitor, YM-254890, on platelet functions and thrombus formation under high-shear stress. Br J Pharmacol 148: 61–69. [PubMed: 16520742]

Uemura T, Takamatsu H, Kawasaki T, Taniguchi M, Yamamoto E, Tomura Y, et al. (2006b). Effect of YM-254890, a specific Galphaq/11 inhibitor, on experimental peripheral arterial disease in rats. Eur J Pharmacol 536: 154–161. [PubMed: 16566917]

van den Bos E, Ambrosy B, Horsthemke M, Walbaum S, Bachg AC, Wettschureck N, et al. (2020). Knockout mouse models reveal the contributions of G protein subunits to complement C5a receptor–mediated chemotaxis. Journal of Biological Chemistry 295: 7726–7742. [PubMed: 32332099]

Van Eps N, Altenbach C, Caro LN, Latorraca NR, Hollingsworth SA, Dror RO, et al. (2018). G_i- and G_s-coupled GPCRs show different modes of G-protein binding. Proceedings of the National Academy of Sciences 115: 2383–2388.

Volkow ND, & McLellan AT (2016). Opioid Abuse in Chronic Pain — Misconceptions and Mitigation Strategies. New England Journal of Medicine 374: 1253–1263. [PubMed: 27028915]

Wang D, Stoveken HM, Zucca S, Dao M, Orlandi C, Song C, et al. (2019). Genetic behavioral screen identifies an orphan anti-opioid system. Science 365: 1267–1273. [PubMed: 31416932]

Williams JT, Ingram SL, Henderson G, Chavkin C, von Zastrow M, Schulz S, et al. (2013). Regulation of μ-opioid receptors: desensitization, phosphorylation, internalization, and tolerance. Pharmacol Rev 65: 223–254. [PubMed: 23321159]

Wirotanseng LN, Kuner R, & Tappe-Theodor A (2013). Gq rather than G11 preferentially mediates nociceptor sensitization. Molecular pain 9: 54–54. [PubMed: 24156378]

Womack MD, & McCleskey EW (1995). Interaction of opioids and membrane potential to modulate Ca2+ channels in rat dorsal root ganglion neurons. J Neurophysiol 73: 1793–1798. [PubMed: 7623080]

Xie W, Samoriski GM, McLaughlin JP, Romoser VA, Smrcka A, Hinkle PM, et al. (1999). Genetic alteration of phospholipase C beta3 expression modulates behavioral and cellular responses to mu opioids. Proc Natl Acad Sci U S A 96: 10385–10390. [PubMed: 10468617]

Yudin Y, & Rohacs T (2018). Inhibitory G(i/O)-coupled receptors in somatosensory neurons: Potential therapeutic targets for novel analgesics. Mol Pain 14: 1744806918763646. [PubMed: 29580154]

Zhuo M, Wu G, & Wu LJ (2011). Neuronal and microglial mechanisms of neuropathic pain. Mol Brain 4: 31. [PubMed: 21801430]

Bullet point summary

What is already known

- Opioids can be effective analgesics, but have unwanted side-effects including addiction, dependence and respiratory depression.

- Opioids activate μ-opioid receptors (MOR) to produce analgesia.

- Propagation of MOR signals may be regulated by other signaling systems.

What this study adds

- Local pharmacological blockade of $G\alpha_{q/11}$ signaling in the spinal cord produces analgesic effects.

- $G\alpha_{q/11}$ blockade enhances the efficacy of systemic morphine administration in mouse models of acute pain.

- $G\alpha_{q/11}$ inhibition suppresses the activity of nociceptor neurons and synergizes with morphine effects on excitability.

What is the clinical significance

- Pharmacological blockage of $G\alpha_{q/11}$ may be a viable strategy for pain management
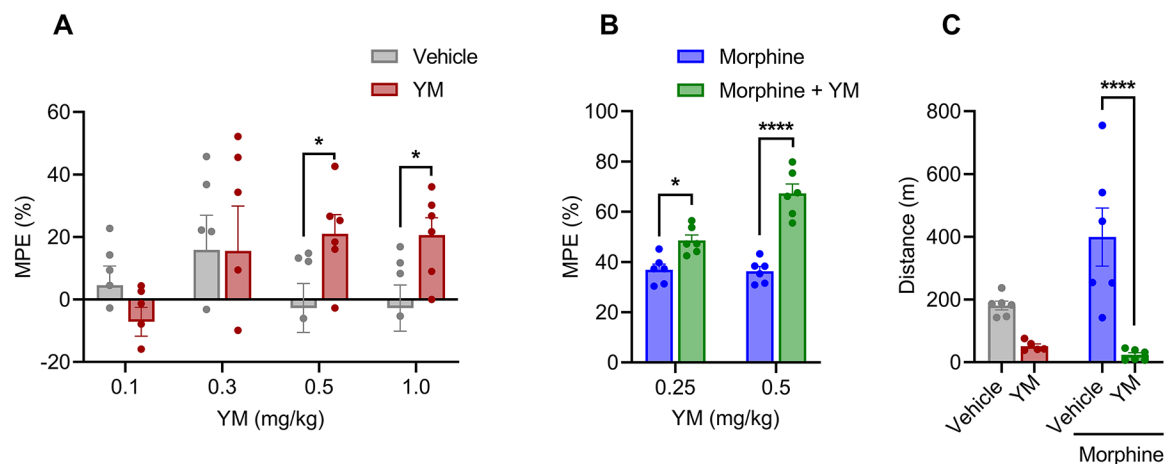
Figure 1: The effect of systemic subcutaneous administration of YM on nociception and locomotion.

A. Dose-response effect of different concentration of subcutaneous YM (0.1, 0.3, 0.5 and 1 mg/kg) and vehicle were tested on hot plate test after 30 min of administration. Unpaired two-tailed Student's t test of YM (0.5 mg/kg) $p = 0.04$; YM (1.0 mg/kg) $p = 0.03$. **B.** Effect of combined administration of subcutaneous YM (0.25 and 0.5 mg/kg) with single dose of subcutaneous morphine (5 mg/kg) on hot plate test after 30 min of morphine administration. YM was administered 10 min before the administration of morphine. Treatment $F_{(1, 10)} = 59.06$, dose $F_{(1, 10)} = 13.21$, interaction $F_{(1, 10)} = 12.08$. Two-way ANOVA with Bonferroni's post hoc test. **C.** Changes in cumulative locomotor activity during 120 min of observation in open field test by subcutaneous administration of YM (0.5 mg/kg), morphine (5 mg/kg), and YM (0.5 mg/kg, 10 min before morphine) with morphine (5 mg/kg), and vehicle treated mice. Treatment $F_{(1, 19)} = 26.02$, effect of morphine $F_{(1, 19)} = 3.71$, interaction $F_{(1, 19)} = 6.2$. Two-way ANOVA with Bonferroni's post hoc test. In all panels statistical analysis was performed combining both sexes and significance was $*p < 0.05$ and $****p < 0.0001$, data sets (mean ± SEM) as analyzed using two-way ANOVA with Bonferroni's multiple comparison test.
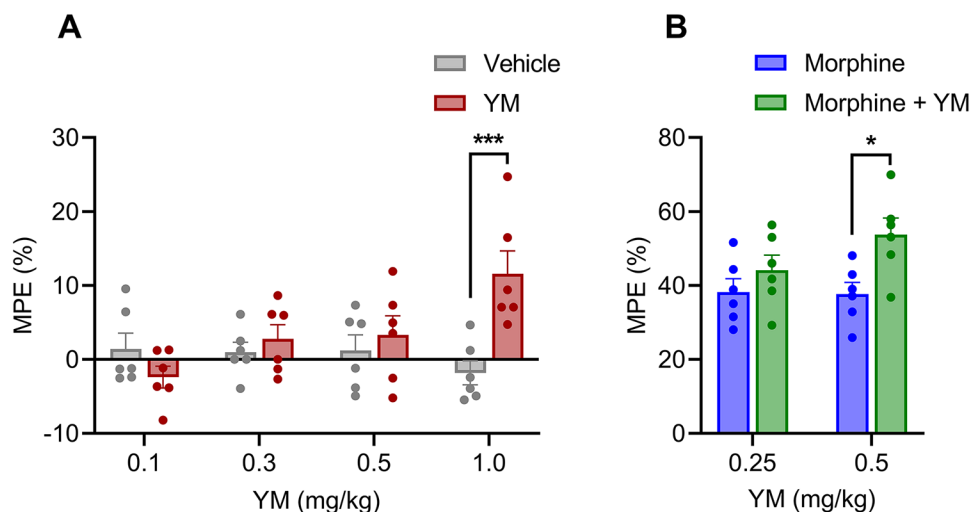
Figure 2: The effect of systemic subcutaneous administration of YM on spinal analgesia.
A. Dose-response effect of different concentration of subcutaneous YM (0.1, 0.3, 0.5 and 1 mg/kg) and vehicle were tested on tail immersion test after 30 min of administration. Treatment $F_{(1, 40)} = 5.14$, dose $F_{(3, 40)} = 2.175$, interaction $F_{(3, 40)} = 5.85$. Two-way ANOVA with Bonferroni's post hoc test. **B.** Effect of combined administration of subcutaneous YM (0.25 and 0.5 mg/kg) with single dose of subcutaneous morphine (5 mg/kg) on tail immersion test after 30 min of administration. YM was administered 10 min before the administration of morphine. Treatment $F_{(1, 20)} = 8.21$, dose $F_{(1, 20)} = 1.38$, interaction $F_{(1, 20)} = 1.75$. Two-way ANOVA with Bonferroni's post hoc test. In all panels statistical analysis was performed combining both sexes and significance was *$p < 0.05$ and **$p < 0.001$, data sets (mean ± SEM) as analyzed using two-way ANOVA with Bonferroni's post hoc test.
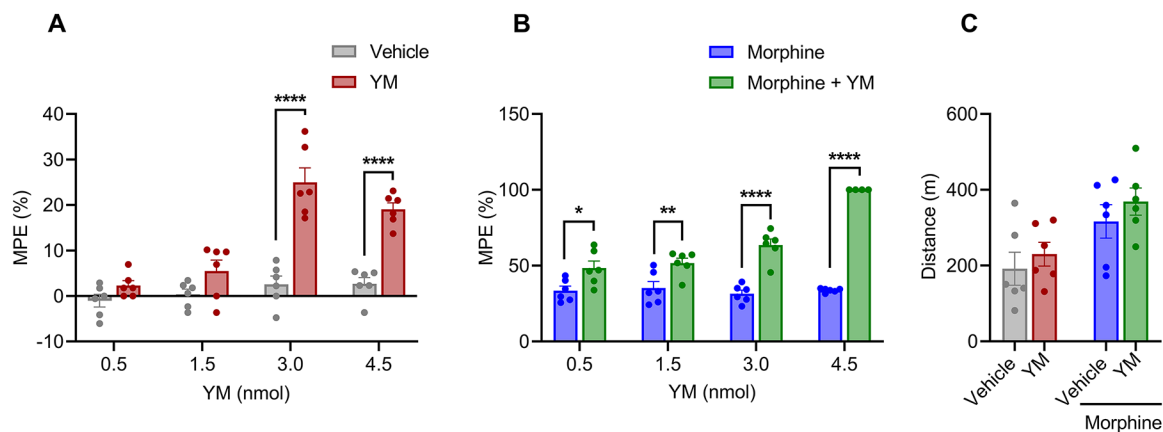
Figure 3: The effect of local intrathecal treatment of YM on spinal analgesia and locomotion.
A. Dose-response effect of different concentration of intrathecal YM (0.5, 1.5, 3.0 and
4.5 nmol) and vehicle were tested on tail immersion test after 30 min of administration.
Treatment $F_{(1, 40)} = 81.67$, dose $F_{(3, 40)} = 22.93$, interaction $F_{(3, 40)} = 12.19$. Two-way
ANOVA with Bonferroni's post hoc test. **B.** Effect of combined administration of intrathecal
YM (0.5, 1.5, 3.0, 4.5 nmol) with single low dose of subcutaneous morphine (2.5 mg/kg) on
tail immersion test after 30 min of administration. YM was administered 10 min before the
administration of morphine. Treatment $F_{(1, 38)} = 185.2$, dose $F_{(3, 38)} = 22.00$, interaction
$F_{(3, 38)} = 22.88$. Two-way ANOVA with Bonferroni's post hoc test. **C.** Changes in
cumulative locomotor activity during 120 min of observation in open field test by intrathecal
administration of YM (3.0 nmol), subcutaneous morphine (2.5 mg/kg), and intrathecal YM
(3.0 nmol, 10 min before morphine) with subcutaneous morphine (2.5 mg/kg) treated mice.
Treatment $F_{(1, 20)} = 1.35$, effect of morphine $F_{(1, 20)} = 11.36$, interaction $F_{(1, 20)} = 0.032$.
Two-way ANOVA with Bonferroni's post hoc test. In all panels statistical analysis was
performed combining both sexes and significance was $*p < 0.05$, $**p < 0.01$, and $****p
< 0.0001$, data sets (mean ± SEM) as analyzed using two-way ANOVA with Bonferroni's
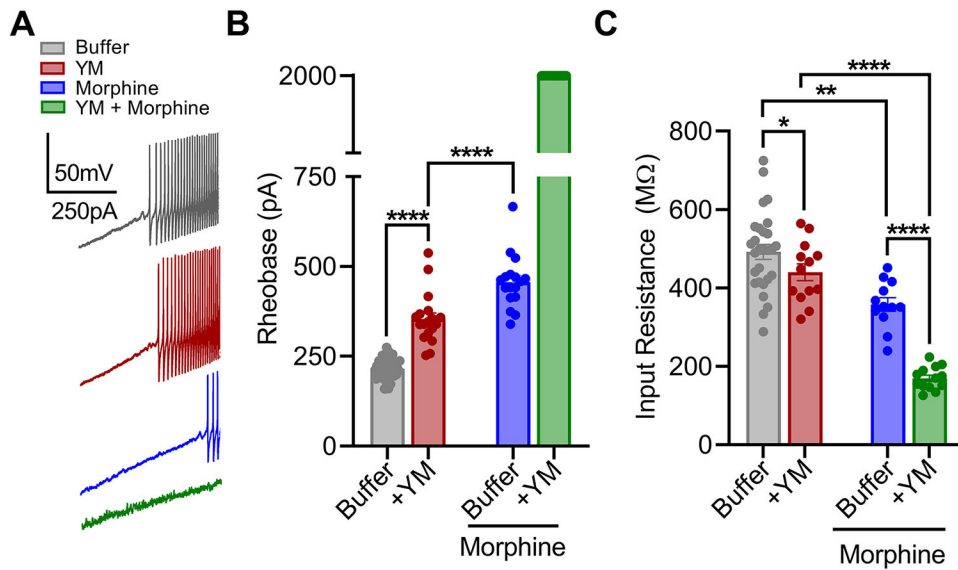multiple comparison test.

Figure 4: The effect of YM treatment on morphine-provoked inhibition of DRG nociceptors.
A. Representative voltage traces from a continuous 0-2 nA ramp stimulation protocol illustrating excitability of a cultured DRG neuron at baseline (black), after bath application of either 1 μM morphine (blue), or 100 nM YM (maroon) followed by both 100 nM YM + 1 μM morphine (green). **B.** Quantification of rheobase from DRG recordings illustrated in A. Co-application of YM and morphine prevented action potential firing throughout the 2 nA ramp protocol in all recordings. YM: $F_{(1, 24)} = 6032$, Morphine: $F_{(1, 24)} = 7591$, Interaction: $F_{(1, 24)} = 4208$. Two-way ANOVA with Bonferroni's multiple comparisons test. **C.** Quantification of resting input resistance at baseline (black), and after bath application of either 1 μM morphine (blue) or 100nM YM (maroon) followed by both 100nM YM + 1 μM morphine (green). YM: $F_{(1, 24)} = 6.636$, Morphine: $F_{(1, 24)} = 172.7$, Interaction: $F_{(1, 24)} = 57.75$. Two-way ANOVA with Bonferroni's multiple comparisons test. Statistical analysis was performed combining both sexes, and significance was $*p < 0.05$, $**p < 0.01$, and $****p < 0.0001$.
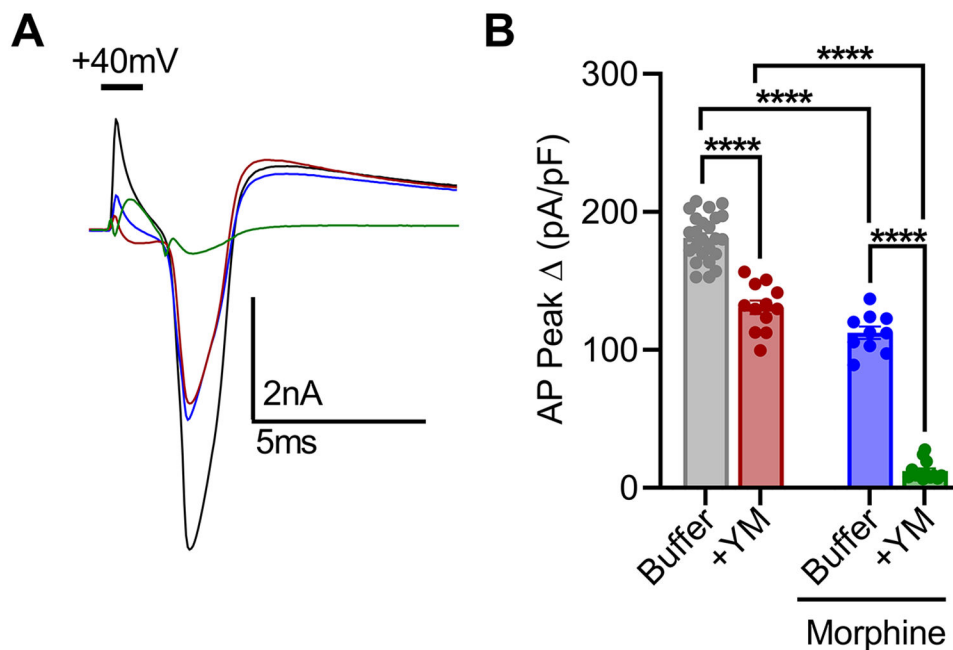
Figure 5: YM and morphine interact to inhibit action potentials of DRG nociceptors.
A. Representative current traces of AP profiles evoked by a 2ms, 40mV voltage-step at baseline (black), and after bath application of either 1μM morphine (blue) or 100 nM YM (maroon) followed by 100 nM YM + 1μM morphine (green). **B.** Quantification of peak AP amplitude normalized to capacitance. Coapplication of YM and morphine greatly inhibited evoked depolarization. YM: $F_{(1, 20)} = 283.0$, Morphine: $F_{(1, 20)} = 633.3$, Interaction: $F_{(1, 20)} = 46.29$. Two-way ANOVA with Bonferroni's multiple comparisons test. Statistical analysis was performed combining both sexes, and significance was $*p < 0.05$, $**p < 0.01$, and $****p < 0.0001$.

Source:

https://www.guidetopharmacology.org/

SN	Hyperlinks (Key Targets and Ligands)	Hyperlink URL
1	GPCR	https://www.guidetopharmacology.org/GRAC/FamilyDisplayForward?familyId=694
2	MOR	https://www.guidetopharmacology.org/GRAC/ObjectDisplayForward?objectId=319&familyId=50&familyType=GPCR
3	YM	https://www.guidetopharmacology.org/GRAC/LigandDisplayForward?ligandId=9335
4	FR	https://www.guidetopharmacology.org/GRAC/LigandDisplayForward?ligandId=9336
5	$G\alpha_q$	https://www.guidetopharmacology.org/GRAC/FamilyDisplayForward?familyId=935
6	GTP	https://www.guidetopharmacology.org/GRAC/LigandDisplayForward?ligandId=1742
7	morphine	https://www.guidetopharmacology.org/GRAC/LigandDisplayForward?ligandId=1627
8	Substance P	https://www.guidetopharmacology.org/GRAC/LigandDisplayForward?ligandId=2098
9	AC	https://www.guidetopharmacology.org/GRAC/FamilyDisplayForward?familyId=257
10	GPR139	https://www.guidetopharmacology.org/GRAC/ObjectDisplayForward?objectId=130
11	PKC	https://www.guidetopharmacology.org/GRAC/FamilyDisplayForward?familyId=286&familyType=ENZYME
12	Design and Analysis	https://bpspubs.onlinelibrary.wiley.com/doi/full/10.1111/bph.14207
13	Animal Experimentation	https://bpspubs.onlinelibrary.wiley.com/doi/10.1111/bph.15232